IOPscience iopscience.iop.org

Home Search Collections Journals About Contact us My IOPscience

The fractal properties of generalised random walks in one dimension

This article has been downloaded from IOPscience. Please scroll down to see the full text article.

1986 J. Phys. A: Math. Gen. 19 2793

(http://iopscience.iop.org/0305-4470/19/14/017)

View the table of contents for this issue, or go to the journal homepage for more

Download details:
IP Address: 129.252.86.83
The article was downloaded on 31/05/2010 at 19:21

Please note that terms and conditions apply.

J. Phys. A: Math. Gen. 19 (1986) 2793-2812. Printed in Great Britain

The fractal properties of generalised random walks in one dimension

J G Powles and G Rickayzen

The Physics Laboratories, University of Kent, Canterbury, Kent CT2 7NR, UK

Received 16 December 1985, in final form 12 May 1986

Abstract. The properties of a simple random walk and random walks with persistence of velocity, in one dimension, are reported. The finite-fractal properties of the walks are obtained, with exact expressions for indefinitely long walks. Remarkably simple expressions are found for the length, $L(\varepsilon)$, at scale ε. Computer simulations of these walks are reported for finite trajectories which help to explain the properties of atomic trajectories in realistic liquids determined by molecular dynamics simulation. Some new molecular dynamics simulations are reported for a typical liquid, its coexisting vapour and the crystal, all at the same temperature. The general form of the fractal properties of the three states of matter are well represented by the present one-dimensional model. Indeed, even the quantitative nature is quite well represented, which suggests that results for random walks in three dimensions will be substantially the same.

1. Introduction

Richardson (1961) suggests that trajectories (or trails) should be analysed using a (variable) scale of length, ε, so that for a given trajectory the length is $L(\varepsilon)$. $L(\varepsilon)$ is measured by stepping *along* the trajectory from the beginning, $\boldsymbol{r}(0)$, until a point is found, $\boldsymbol{r}(t_1)$, for which $|\boldsymbol{r}(t_1)-\boldsymbol{r}(0)|=\varepsilon$ *for the first time* and repeating this process, i.e. $|\boldsymbol{r}(t_{n+1})-\boldsymbol{r}(t_n)|=\varepsilon$, until the end of the trajectory is reached (usually adding a suitable fraction of ε at the end). Richardson noted that many trajectories are self-scaling in the sense that

$$L(\varepsilon)\propto\varepsilon^{-\alpha} \tag{1.1}$$

where α is a constant, in general non-integral, for a substantial range of ε.

More recently this idea has been elegantly exploited by Mandelbrot (1982) who pointed out that the coefficient $(1+\alpha)$ may be interpreted as a 'dimension' which, in general, is not integral (Hausdorff 1919) and which he calls a fractal dimension (which we call D_f).

This procedure was first applied to the trajectories of atoms in a realistic liquid (actually a computer-simulated liquid) by Powles and Quirke (1984).

Of course for ε small, say much smaller than the mean free path ε_v, $L(\varepsilon)$ approaches the contour length of the trajectory, L_c (which is a function of T, where T is the total time for the trajectory). Thus for $\varepsilon\to 0$ we have from (1.1) that $\alpha\to 0$ ($D_f\to 1$).

It was pointed out by Rapaport (1984, 1985), who used a hard-sphere liquid, that our simulations were too short to achieve the expected limiting value of α for long T and that $\alpha\to 1$ ($D_f\to 2$) for long enough trajectories for this liquid.

0305-4470/86/142793+20$02.50 © 1986 The Institute of Physics

Powles (1985) then carried out longer simulations for his liquid and found values of α closer to unity but that the convergence is extraordinarily slow, possibly because the velocity autocorrelation functions have a 'long-time tail'. This has recently been investigated by Toxvaerd (1985) who compared the behaviour of model liquids with and without long-time tails. Powles (1985) suggested a generalisation of the fractal analysis of physical trajectories in which α depends on the trajectory length, or maximum scale, $\varepsilon_{\max}$, i.e. $\alpha\ (\varepsilon_{\max})$, and gave an elementary analysis of this function which appears to explain the observed slow convergence. This was called finite-fractal analysis. A similar approach has been suggested by Takayasu (1982) who called $[\alpha(\varepsilon)+1]$ the 'differential fractal dimension'.

This analysis has recently been applied to the trajectories of the mobile ions in superionic conductors by Vashishta *et al* (1985) who found similar finite-fractal curves but that the convergence of α to unity is relatively rapid for this system and establishes, with reasonable accuracy, that $\alpha(\infty)=1$. A similar result has been found for two-dimensional molecular motion by Kalia *et al* (1985).

The problem remains as to the form of $L(\varepsilon)/L_c$ for fluid and quasifluid systems and how this depends on more familiar parameters of the atomic motion and, indeed, whether this analysis demands the introduction of other more subtle parameters of the motion. It has been asserted recently (Toxvaerd 1986) that it is sufficient to know the velocity time autocorrelation function, $\phi_v(t)$, but in our opinion this is still only an approximate theory for $\alpha(\varepsilon)$.

It therefore seemed that it might be instructive to do a finite-fractal analysis for some simple, well defined and exactly analysable systems. In the following we do this for the simple random walk and some generalisations. This analysis throws light on the physical nature of realistic trajectories and suggests what the behaviour of the more interesting and important trajectories in the real world of three dimensions might be.

2. Simple random walk in one dimension

2.1. Elementary properties of the model

The simplest random walk is one in which the particle travels at constant speed v, either in the positive or negative direction, a distance l for fixed time intervals τ. If the velocity is $+v$ (or $-v$) in a given step, then it is $\pm v$ in the next step with equal probability. This is a well known model for diffusional motion which is discussed in detail by Chandrasekhar (1943). The mean-square distance travelled in n steps is readily obtained:

$$x[n\tau] = x[(n-1)\tau] \pm l$$

with equal probability, so

$$\begin{aligned}\langle x^2[n\tau]\rangle &= \tfrac{1}{2}\langle\{x[(n-1)\tau]+l\}^2\rangle + \tfrac{1}{2}\langle\{x[(n-1)\tau]-l\}^2\rangle \\ &= \langle x^2[(n-1)\tau]\rangle + l^2\end{aligned}$$

but $\langle x^2(0)\rangle = 0$, therefore

$$\langle x^2(n\tau)\rangle / l^2 = n. \tag{2.1}$$

Chandrasekhar shows that, for large n, the probability distribution of x, $p(x, t)$, obeys the one-dimensional diffusion equation

$$D\frac{\partial^2 p(x,t)}{\partial x^2} = \frac{\partial p(x,t)}{\partial t} \tag{2.2}$$

with the diffusion constant D (not to be confused with the fractal dimension D_f) given by

$$D = l^2/2\tau. \tag{2.3}$$

The velocity autocorrelation function, $\phi_v(t)$, for this model is readily calculated since if v is $+v$ (or $-v$) at any given step it is equally likely to be $\pm v$ in any subsequent step, so correlation is completely lost in one step. Thus

$$\phi_v(t) \equiv \langle v(t')v(t'+t)\rangle / \langle v^2(t')\rangle$$

(t' for lattice points)

$$\phi_v(t) = \begin{cases} 1 & \text{for } 0 < t < \tau \\ 0 & \text{for } t > \tau. \end{cases} \tag{2.4}$$

The velocity correlation time, τ_v, is defined as

$$\tau_v \equiv \int_0^\infty \phi_v(t)\, \mathrm{d}t. \tag{2.5}$$

For this model $\tau_v = \tau$ and we note that $\phi_v(t)$ is short-ranged.

2.2. *Finite-fractal properties*

We now calculate $L(\varepsilon)$ where $\varepsilon = kl$, k being a positive integer for a walk of n steps. Firstly we have, clearly,

$$L_c = nl = lT/\tau \qquad L(l) = nl \qquad \text{i.e. } L(l)/L_c = 1. \tag{2.6}$$

Clearly, also, $L(l/j)/L_c = 1$, where j is any positive integer.

For a given trajectory of elapsed time T we have the basic relation

$$L(\varepsilon) = \varepsilon(T/\langle t(\varepsilon)\rangle) \tag{2.7}$$

where $\langle t(\varepsilon)\rangle$ is the mean time for the particle to travel from a given point on the trajectory to one a distance ε away, *for the first time.* For ε small and T large the value of $\langle t(\varepsilon)\rangle$ is precise but the accuracy decreases as ε increases.

We now evaluate $L(\varepsilon)$ for an indefinitely long trajectory for which $\langle t(\varepsilon)\rangle$ can be obtained exactly for all ε. We shall discuss $L(\varepsilon)$ for real, i.e. finite, trajectories shortly.

We write (2.7) in the form

$$L(\varepsilon)/L_c = (\varepsilon/l)/[\langle t(\varepsilon)\rangle/\tau]. \tag{2.7'}$$

For $\varepsilon = 2l$ we get the pattern given in figure 1. Note that the paths which get to $\pm 2l$ for the first time must be discarded (or rather not counted) for subsequent times. This first occurs at $t = 2\tau$ and then at every interval of 2τ *ad infinitum.* This is indicated on the diagrams by a bold dot. Thus the probability of getting to $2l$ in time 2τ is $\frac{1}{2}$, in time 4τ is $\frac{1}{4}$, and so on. For $t > 4\tau$ the pattern repeats, so that

$$\langle t(2l)\rangle/\tau = (2\times\tfrac{1}{2} + 4\times\tfrac{1}{4} + 6\times\tfrac{1}{8} + \ldots)/(\tfrac{1}{2} + \tfrac{1}{4} + \ldots) = 4$$

i.e.

$$L(2l)/L_c = \tfrac{1}{2}.$$

For $\varepsilon = 3l$ we get a similar diagram to figure 1, the *pattern* repeats after $t = 5\tau$ and the series are readily summed. We find

$$\langle t(3l)\rangle/\tau = 9 \qquad L(3l)/L_c = \tfrac{1}{3}.$$

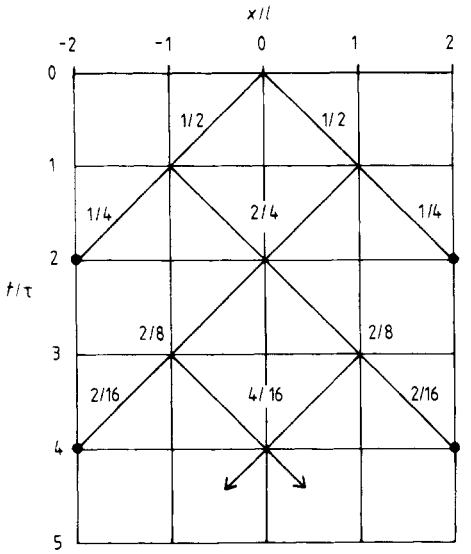

Figure 1. The evaluation of probabilities for the random walk of § 2 for the calculation of the mean first passage time, $\langle t(\varepsilon)\rangle$, for $\varepsilon/l = 2$. The full dots indicate the 'absorption' of probability when a trajectory gets to $x = \pm\varepsilon$ for the first time. The pattern repeats after $t = 2\tau$ with period 2τ.

For $\varepsilon = 4l$, the diagram is more complex, there are no obvious repeats and the series are slower to converge. However, it is easy to convince oneself that $\langle t(4l)\rangle/\tau = 16$. There seems no point in proceeding further by exact analysis since it is quite straightforward to compute $\langle t(\varepsilon)\rangle$ to any desired accuracy for $\varepsilon = kl$ and k not too large. The first contribution to $\langle t(kl)\rangle$ is for $t = k\tau$ when the probabilities are simply proportional to the binomial coefficients. Thereafter the probabilities for $t = (k+2)\tau$ are readily computed by simple recursive relations. We then soon conclude that

$$L(kl)/L_c = 1/k \tag{2.8}$$

exactly.

An asymptotic relation for large k is readily obtained from the diffusion limit. We solve (2.2) with the boundary conditions

$$p(x, t) = \delta(x) \qquad \text{for } t = 0$$

$$p(\pm\varepsilon, t) = 0 \qquad \text{for all } t.$$

The latter conditions arise because we must take the first occurrence of the interval ε as we step along the trajectory. It corresponds to diffusion with totally absorbing barriers at $x = \pm\varepsilon$ (see figure 1) but with the motion of the surviving particles unaffected, i.e. $D(=l^2/2\tau)$ is a constant independent of time.

The general solution of (2.2) is

$$p(x, t) = \sum (A_k \cos kx + B_k \sin kx) \exp(-k^2 Dt).$$

The constraints require that

$$B_k = 0 \qquad \sum A_k \cos k\varepsilon \exp(-k^2 Dt) = 0 \qquad \text{for all } t$$

i.e. $k = (n+\frac{1}{2})\pi/\varepsilon$, n integer including 0, so that

$$\sum A_n \cos(n+\tfrac{1}{2})\pi x/\varepsilon = \delta(x)$$

whence $A_n = 1/\varepsilon$ and so

$$p(x, t) = (1/\varepsilon) \sum_{n=0}^{\infty} \cos[(n+\tfrac{1}{2})\pi x/\varepsilon] \exp[-(n+\tfrac{1}{2})^2 \pi^2 Dt/\varepsilon^2].$$

The fraction of particles unabsorbed at time t, $f(t)$, is therefore

$$f(t) = (4/\pi) \sum (-1)^n (2n+1)^{-1} \exp[-(n+\tfrac{1}{2})^2 \pi^2 Dt/\varepsilon^2].$$

We require the probability that a particle gets to $\pm\varepsilon$ at time t, which we call $p(t, \varepsilon)$ (not to be confused with $p(x, t)$) with

$$p(t, \varepsilon) = -\mathrm{d}f/\mathrm{d}t = (\pi D/\varepsilon^2) \sum (-1)^n (2n+1) \exp[-(n+\tfrac{1}{2})^2 \pi^2 Dt/\varepsilon^2].$$

Finally

$$\langle t(\varepsilon) \rangle = \int_0^{\infty} \mathrm{d}t\, tp(t, \varepsilon) = [16\varepsilon^2/(\pi^3 D)] \sum_{n=0}^{\infty} (-1)^n (2n+1)^{-3}$$

i.e.

$$2D\langle t(\varepsilon) \rangle/\varepsilon^2 = (32/\pi^3)\{1 - 3^{-3} + 5^{-3} - \ldots\} = 1$$

or $\varepsilon^2 = 2D\langle t(\varepsilon) \rangle$ (see Fürth 1917). This may be compared with $\langle x^2 \rangle = 2Dt$. Hence, using (2.7) and substituting for D, we have

$$L(\varepsilon)/L_c \to 1/(\varepsilon/l)$$

in the diffusion limit, which is exactly the same as (2.8). Hence for this model we have

$$\alpha \equiv -\mathrm{d}[\ln L(\varepsilon)]/\mathrm{d}[\ln \varepsilon] = 1$$

i.e. $D_f = 2$ for all $\varepsilon = kl$, k a positive integer.

A formal proof of these results is given in appendix 2. However, this result is only true for infinite trajectories, i.e. for $T \to \infty$ and $L_c \to \infty$, since we have taken the limiting values of $\langle t(\varepsilon) \rangle$.

It is instructive to obtain the corresponding results for actual finite trajectories. This is readily done on the computer since a trajectory can be generated very rapidly by the use of pseudo-random numbers. Having obtained the trajectory, $L(kl)$ can be calculated immediately. This is extremely fast because one can use integer arithmetic for this model. It is convenient to use, $T/\tau = 2^m$, with m integer.

The results of such a computation for one seed for a trajectory of increasing length are given in table 1 and figure 2.

The entries in the table show how $[L(kl)/L_c]^{-1}$ tends to k as T increases. When k is small the convergence is rapid because $L(kl)$ includes a large number of steps of length $\varepsilon = kl$. As k increases for a given trajectory, the number of steps included in $L(kl)$ decreases and it becomes more and more dependent on the particular trajectory. Notice that the maximum value of ε, ε_{max}, which is of course also trajectory-sensitive, is much less than L_c although it can be, and usually is, considerably larger than the end-to-end length, L_{ete}, of the particular trajectory. The *mean* value of L_{ete} is $\langle |x(T)| \rangle$. A rough estimate of ε_{max} is $\langle x^2(T) \rangle^{1/2}$. These are also given in table 1.

It is also easy to confirm the form of $\langle x^2 \rangle$ given in (2.1) (see table 2) and of $\phi_v(t)$ given in (2.4) and these are reproduced to good accuracy even for quite short trajectories.

The results in table 1 and figure 2 illustrate the slow convergence of the fractal properties analysis of the actual finite trajectories to the limiting values, (2.8), for an infinite trajectory. They have to be enormously longer in time T than τ_v, depending on the value of ε. For example, for the shortest trajectory quoted we have a very poor result for even $\varepsilon/l = 2$ whereas $T = 64\tau_v$. This slow convergence with increasing length

Table 1. Values of $[L(kl)/L_c]^{-1}$ for trajectories with $n = 2^m$ steps.

k	$L_c/l = T/\tau = 64$	128	256	512	1024	2048	4096
1	1	1	1	1	1	1	1
2	1.60	1.73	2.10	2.15	2.16	2.16	2.06
3	2.29	2.78	3.12	3.28	3.05	3.15	2.98
4	2.29	3.37	4.13	3.71	4.00	3.94	3.87
5	2.67	4.27	5.12	4.13	4.00	4.57	4.53
6	4.00	4.92	6.73	5.69	6.10	6.40	6.08
7	3.56	4.00	6.73	6.56	6.83	7.11	6.80
8		12.80	25.6	12.2	11.64	9.48	8.03
9		12.80	25.6	17.1	13.12	9.84	9.18
10		12.80	25.6	15.1	12.2	10.67	10.95
11		10.67	21.3	13.5	11.4	10.8	11.9
12		9.14	18.3	12.2	10.7	12.8	12.6
13		8.00	16.0	25.6	12.8	16.8	13.7
14		7.11	14.2	23.3	12.8	15.5	12.7
15				21.3	12.2	14.4	11.9
16				19.7	18.3	23.3	15.2
17				18.3	17.7	21.8	22.3
18				17.1	17.1	20.5	21.1
				⋮	⋮	⋮	⋮
ε_{max}/l	7	14	14	25	26	47	47
$n^{1/2}$	8	11.3	16	22.6	32	45.3	64
L_{ete}/l	4	10	10	6	24	8	14
$\|x(T)\|/l$	6.4	9.0	12.8	18.0	25.5	36	51

of trajectory, in spite of the short-ranged velocity autocorrelation function, is similar to that observed for realistic trajectories (e.g. Powles 1985). It may be contrasted with the situation for diffusion, where the exact result for an infinite trajectory is given in (2.1), i.e.

$$\langle x^2\rangle(t)/l^2 = t/\tau.$$

For our shortest trajectory, $T = 64\tau$, we find the values given in table 2, which may be contrasted with the first column of table 1.

However this model is, as already noted, far from realistic. In particular we have a sharp change from $\alpha = 0$ for $\varepsilon = l/k$ to $\alpha = 1$ for $\varepsilon = kl$, $k = 1, 2, 3, \ldots$. For realistic trajectories the changeover is smooth and gradual (see figure 9).

We now consider a generalisation of this random walk.

3. Random walks with persistence and antipersistence of velocity

3.1. Elementary properties of the model

The speed is still constant at v and changes at fixed intervals τ. However if the velocity is $+v$ (or $-v$) in a given interval, it is $+v$ (or $-v$) with probability p in the subsequent interval and $-v$ (or $+v$) with probability $q = 1 - p$. This is a Markov process. For $p = \frac{1}{2}$ we recover the simple walk of § 2.

It is elementary to determine the velocity autocorrelation function. It is

$$\phi_v(k\tau < t < (k+1)\tau) = (2p-1)^k \qquad k = 0, 1, \ldots \tag{3.1}$$

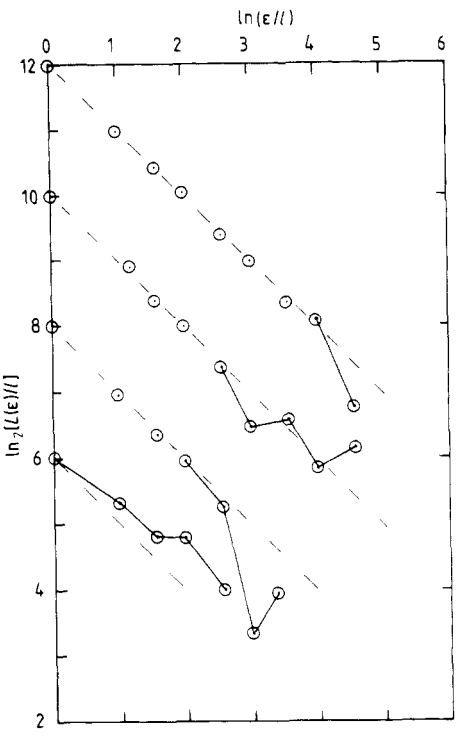

Figure 2. The computed finite-fractal data for the simple random walk for the trajectories in table 1. The broken lines are for an infinite trajectory, shifted for finite L_c. The values of $\ln_2[L(\varepsilon)/l]$ for $\ln_2(\varepsilon/l)=0$ correspond to the values of L_c. For clarity only values for octaves and approximate semi-octaves of ε/l are plotted and the lines joining the points are to aid the eye.

Table 2. Mean-square distance diffused in time t for the trajectory of table 1 with $T/\tau=64$.

t/τ	1	2	3	4	8	16
$\langle x^2(t)\rangle/l^2$	1	2.08	3.18	4.29	8.79	16.9

and

$$\tau_v/\tau = 1/[2(1-p)]. \tag{3.2}$$

We define a mean free path, ε_v, again by $\varepsilon_v = v\tau_v$.

For $p>\frac{1}{2}$, $\phi_v(t)$ decays in steps and for $p<\frac{1}{2}$, $\phi_v(t)$ is oscillatory in steps. In particular, for $p=1$

$$\phi_v(t)=1 \qquad \tau_v/\tau=\infty$$

i.e. free flight, and for $p=0$

$$\tau_v/\tau=\tfrac{1}{2} \qquad \phi_v(t) \text{ is a 'square wave'.}$$

For $p\to 1$

$$\phi_v(t)\to\exp(-t/\tau_v). \tag{3.3}$$

Before investigating $L(\varepsilon)$ we give an elementary deduction of $\langle x^2\rangle(t)$. The diagram required is shown in figure 3. The 'flow' of probability is more complex than for figure 1 because we have to keep track of the sign of the velocity in the previous step.

For small values of $t = n\tau$ we can show that

$$\begin{aligned}
\langle x^2(n\tau)\rangle/l^2 &= 1 && \text{for } n=1\\
&= 2+4(p-\tfrac{1}{2}) && \text{for } n=2\\
&= 3+8(p-\tfrac{1}{2})+8(p-\tfrac{1}{2})^2 && \text{for } n=3\\
&= 4+12(p-\tfrac{1}{2})+16(p-\tfrac{1}{2})^2+16(p-\tfrac{1}{2})^3 && \text{for } n=4\\
&= 5+16(p-\tfrac{1}{2})+24(p-\tfrac{1}{2})^2+32(p-\tfrac{1}{2})^3+32(p-\tfrac{1}{2})^4 && \text{for } n=5.
\end{aligned}$$

We postulate that

$$\langle x^2(n\tau)\rangle l^2 = n+2(n-1)(2p-1) +2(n-2)(2p-1)^2+2(n-3)(2p-1)^3+\ldots \qquad \text{to } n \text{ terms}$$

i.e.

$$\langle x^2(n\tau)\rangle/l^2 = n\left(\frac{p}{1-p}\right)-\frac{(2p-1)}{2(1-p)^2}[1-(2p-1)^n] \qquad n=0,1,2.\ldots. \tag{3.4}$$

This result is shown to be exact in appendix 1.

Alternatively we can calculate $\langle x^2\rangle$ from actual trajectories, calculated as in § 2, by a modest elaboration of the program. For this we used a trajectory with an elapsed time of $T/\tau = 2^{19} = 542\,288$ steps, which corresponded to the limit of the fast store available. The results correspond to equation (3.4) to the computational accuracy.

For large n (3.4) yields

$$\langle x^2(n\tau)\rangle/l^2 \to n\left(\frac{p}{1-p}\right)-\frac{(2p-1)}{2(1-p)^2} \qquad p \neq 1. \tag{3.5}$$

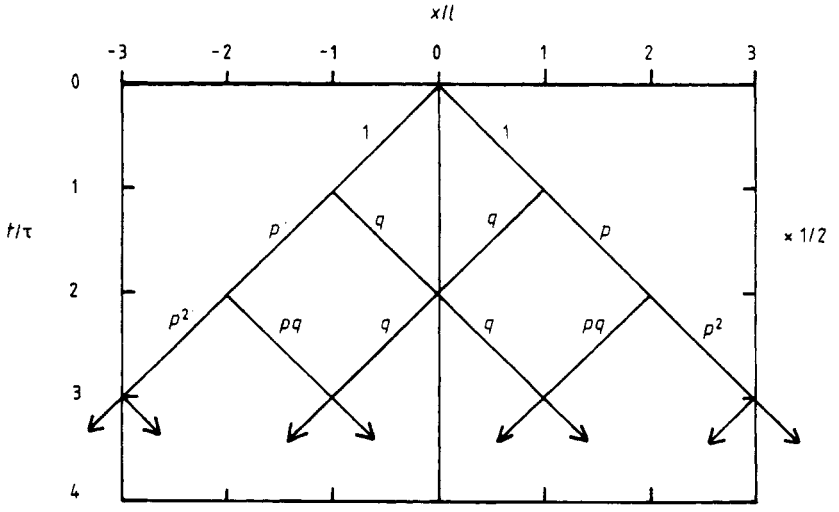

Figure 3. Diagram for the evaluation of $\langle x^2\rangle$ for the random walk with persistence of velocity (§ 3).

This may be compared with the standard limiting form for diffusion in one dimension

$$\langle x^2 \rangle = 2Dt + \gamma \qquad t \to \infty$$

so that

$$D(p) = \left(\frac{l^2}{2\tau}\right)\left(\frac{p}{1-p}\right) \qquad \gamma = -\frac{(2p-1)}{2(1-p)^2} l^2. \tag{3.6}$$

As expected $D(p \to 1) \to \infty$ and $D(p \to 0) \to 0$. For realistic liquids γ is positive (Rahman 1964). The result for $D(p)$ is given by van Beijeren (1982) (his equation 4.21).

3.2. The finite-fractal properties of this model

We now calculate $L(\varepsilon)$. It is obvious that, for $\varepsilon = l$,

$$L(l)/L_c = 1 \qquad \text{for all } p. \tag{3.7}$$

For $\varepsilon = 2l$ we get a generalisation of figure 1 which is given in figure 4. The pattern repeats for $t = k\tau$, k even, and

$$\frac{\langle t(2l) \rangle}{\tau} = \frac{2p + 4pq + 6pq^2 + \ldots}{(p + pq + pq^2 + \ldots)} = 2/p$$

so that

$$L(2l)/L_c = p. \tag{3.8}$$

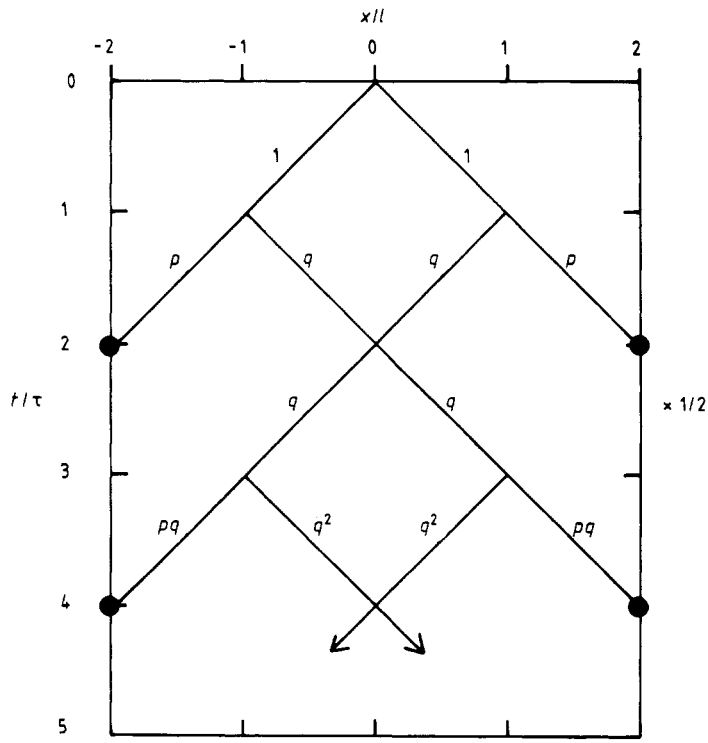

Figure 4. Diagram for the evaluation of $\langle t(2l) \rangle$ for trajectories with persistence of velocity.

For $\varepsilon > 2l$ this becomes too tedious. However, again for large ε we can use the diffusion limit as in § 2 but with $D(\frac{1}{2})$ replaced by $D(p)$ from (3.6) so that

$$\langle t(\varepsilon)\rangle/\tau \to (\varepsilon/l)^2(1-p)/p$$

and, cf (2.7′),

$$L(\varepsilon)/L_c \to (\varepsilon/l)^{-1}p/(1-p). \tag{3.9}$$

Hence for $\varepsilon/l \to \infty$, $\alpha \to 1 (D_f \to 2)$ for any p, except $p = 0$ or 1.

The general result can be readily calculated to any desired accuracy for any p by direct computation of a trajectory. We have done this for a trajectory of 2^{19} steps. The exact result (3.8) is readily tested. The limiting result (3.9) is more difficult to test numerically for $p \neq \frac{1}{2}$ because of slow convergence, in part due to the shift occasioned by the factor $p/(1-p)$ in (3.9), but there seems little doubt that this asymptotic value is approached. The numerical results are given in figure 5 for a number of values of p from $\frac{1}{32}$ to $\frac{31}{32}$.

The intercepts on the line $\ln_2(L(\varepsilon)/L_c) = 0$ for $p > \frac{1}{2}$ and on the line $\ln_2(\varepsilon/l) = 0$ for $p < \frac{1}{2}$ correspond to the asymptotic result (3.9). The full point on the curves for $p > \frac{1}{2}$ corresponds to $\varepsilon = \varepsilon_v = l\tau_v/\tau$ (cf (3.2)).

Having checked the general behaviour by computation we now obtain, by elementary methods, an expression for $L(\varepsilon)$ which is exact.

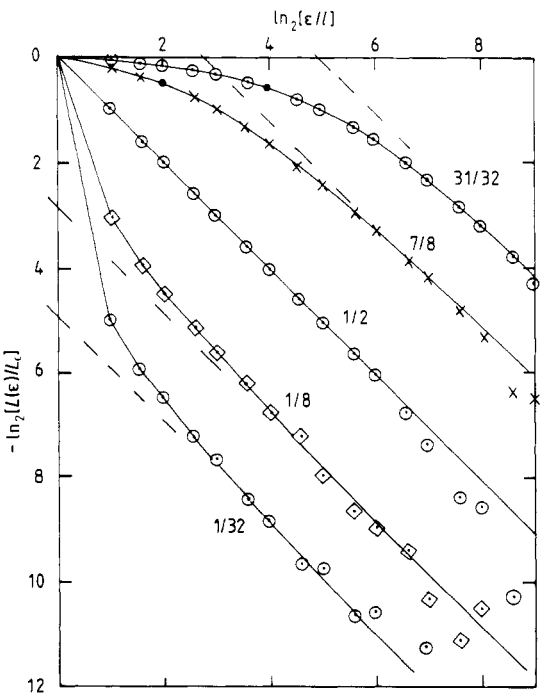

Figure 5. Computed values of $L(\varepsilon)/L_c$ as a function of ε, plotted logarithmically (to base 2) for trajectories of elapsed time $2^{19}\tau$ for various persistences (and antipersistences) of velocity corresponding to the values of p adjacent to the curves. The full straight lines join the points for $\varepsilon/l = 2^m$ and 3×2^m given by equation (3.12). The intercepts on the axes correspond to the limiting straight lines given by equation (3.9). The full points on the curves for $p > \frac{1}{2}$ correspond to $\varepsilon = \varepsilon_v$.

We have the exact results (3.7) and (3.8) and the asymptotic result (3.9). We now obtain the result for $L(3l)$ to order q^2. The diagram for this is given in figure 6. The actual values are one-half times those given, for convenience. Only one-half of the diagram is shown, as it is symmetrical about $x=0$. The diagram terminates at $t=11\tau$ so that an exact result is obtained to order q^2. The result is

$$\langle t(3l)\rangle/\tau = 3(1+2q+2q^2)+O(q^3)$$

so that

$$L(3l)/L_c = (1+2q+2q^2+\ldots)^{-1}.$$

If this series continues in like manner we have

$$L(3l)/L_c = p/(2-p). \tag{3.10}$$

Similarly for $L(4l)$ the lattice terminates at $t=16\tau$ and we find

$$L(4l)/L_c = (1+3q+3q^2+\ldots)^{-1}.$$

Again if this series continues we have

$$L(4l)/L_c = p/(3-2p). \tag{3.11}$$

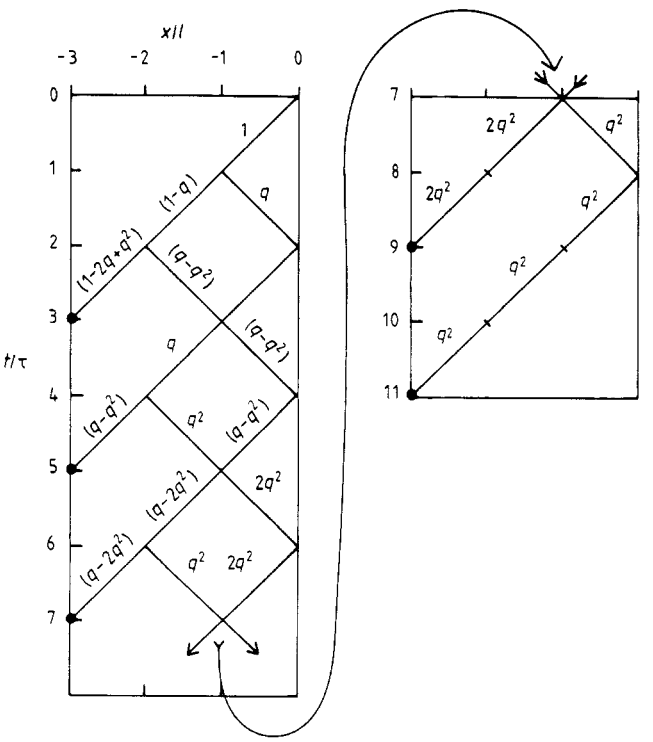

Figure 6. The diagram for calculating $\langle t(3l)\rangle$ but only retaining values of the probabilities to order q^2. Note that the ladder terminates at $t=11\tau$. Only half of the symmetric diagram is given. Actual probabilities are one-half of those indicated.

If (3.7), (3.8), (3.10) and (3.11) continue and are consistent with the asymptotic limit (3.9) we have

$$L(nl)/L_c = p/[n(1-p)+(2p-1)] \qquad n \text{ integral.} \tag{3.12}$$

Putting (3.12) in canonical form we have

$$L(\varepsilon)/L_c = [p/(1-p)][(\varepsilon/l)+(2p-1)/(1-p)]^{-1}. \tag{3.12'}$$

By comparison with the simulation results given in figure 5 and bearing in mind that the scatter for large ε (note the logarithmic scale) may be ignored in view of (3.9), which is also consistent with (3.12), we conclude that (3.12) is exact whether q is small or not. Indeed it is true even for $q \to 1$ ($p \to 0$)! It is a remarkably simple result.

It is also useful to express (3.12) in terms of ε_v when

$$L(\varepsilon)/L_c = [2-(l/\varepsilon_v)]/[(\varepsilon/\varepsilon_v)+2-2(l/\varepsilon_v)]. \tag{3.12''}$$

The relations (3.12) are shown to be exact in appendix 2.

3.3. The special case $p \to 1$

In the limit $\varepsilon_v \gg l$ (i.e. $p \to 1$) we have the even simpler result that

$$L(\varepsilon)/L_c \to 1/(\varepsilon/2\varepsilon_v + 1). \tag{3.13}$$

In this case the finite-fractal properties are entirely determined by the value of the velocity autocorrelation time only—apart from the trivial quantity $\langle v \rangle$.

It is readily proved by elementary methods that result (3.13) is exact. For $p \to 1$, we have $q \to 0$. Draw a 'ladder' as in figure 4 for a few values of $\varepsilon = nl$, say $n = 2$, 4 and 6, but retain probabilities only to order q. It is then easy to see that the general form of the ladder for $\varepsilon = nl$ from $t = n\tau$ onwards is as in figure 7. The first 'absorption' is at $t = n\tau$ with probability $[1-(n-1)q]$. The subsequent absorptions are at $t = (n+2)\varepsilon$, $(n+4)\tau \ldots$, the probability is always q and there are n absorptions in total. Hence

$$\langle t(nl) \rangle/\tau = n[1-(n-1)q] + q[(n+2)+(n+4)+\ldots(n-1) \text{ terms}]$$

$$= n[1+(n-1)q] \qquad \text{to order } q(n^2q < 1).$$

Thus for $n \gg 1$

$$L(\varepsilon)/L_c = (1+nq)^{-1} \qquad \text{to order } q.$$

But $n = \varepsilon/l$ and $2\varepsilon_v = l/q$ exactly. Therefore

$$L(\varepsilon)/L_c = (1+\varepsilon/2\varepsilon_v)^{-1} \qquad \text{for } q \to 0$$

which is (3.13).

We recall that for $p \to 1$, $\phi_v(t)$ is exponential (cf (3.3)) and $\tau_v/\tau \to \infty$.

The slope, $\alpha(\varepsilon)$, of the finite-fractal plot for this special case, (3.13), is given by

$$\alpha(\varepsilon) = \frac{(\varepsilon/2\varepsilon_v)}{(\varepsilon/2\varepsilon_v+1)}. \tag{3.14}$$

Notice that $\alpha(\varepsilon \to 0) \to 0$ and $\alpha(\varepsilon \to \infty) \to 1$ and the transition is smooth and gradual, cf the curve for $p = \frac{31}{32}$ in figure 5.

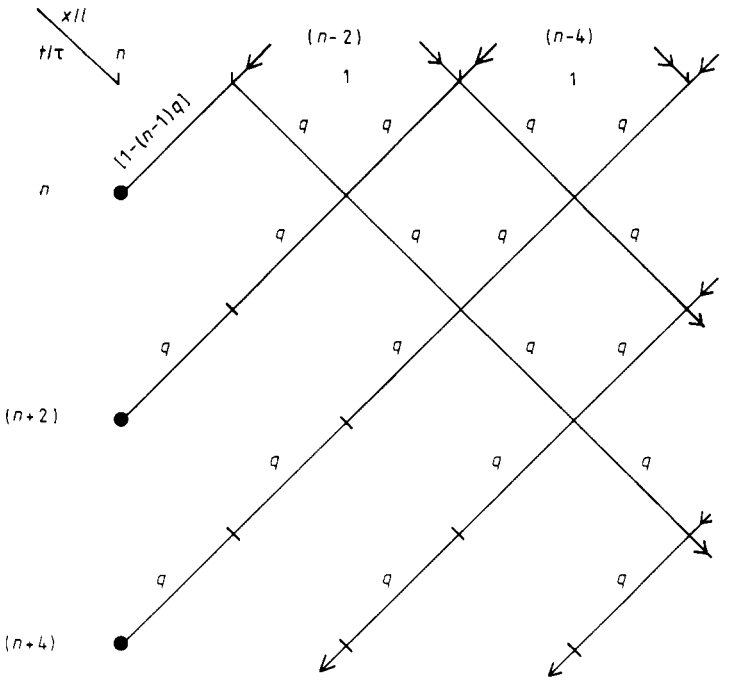

Figure 7. Diagram for the proof of equation (3.13). The probabilities should all be multiplied by one-half. Only part of half the diagram, which is symmetrical about $x = 0$, is shown. It continues upwards, downwards and to the right to an extent depending on the value of n.

$\alpha(\varepsilon)$ is within 5% of its asymptotic value of unity for $\varepsilon/2\varepsilon_v \simeq 19$. Let us estimate the length of the trajectory required to show that the limiting slope is unity to 5%. To a very rough approximation

$$\varepsilon_{\max}^2 \simeq \langle x^2(T)\rangle = 2D(p \to 1)T = 2v^2\tau_v T$$

and $\varepsilon_v = v\tau_v$. Thus for $\varepsilon/2\varepsilon_v \simeq 19$ we require

$$T \simeq 700\tau_v.$$

In a usual simulation one would use a computational time step of, say, $\Delta t = \tau_v/20$ so that we require

$$T \simeq 14\,000\Delta t \qquad \text{i.e. } 14\,000 \text{ time steps}$$

which is quite long by usual standards. But this is for a $\phi_v(t)$ which is exponential, which is short-ranged in the sense that it has no algebraic long-time tail. For a $\phi_v(t)$ with a long-time tail one would surely have to simulate the liquid for at least a factor ten longer (the addition of a tail increases τ_v but not in proportion). Hence for a realistic liquid we estimate that one may require the order of 150 000 time steps. This seems therefore to be an explanation of why Powles and Quirke (1984), Powles (1985) and Toxvaerd (1985) did not observe the limiting value of α. Rapaport (1984) for the hard-sphere fluid was able to get much nearer to the asymptotic value of α, although the simulations required were still very long.

For what appears to be this model for 'Brownian motion', Takayasu (1982) finds, by a quite different and presumably exact analysis, the same formula (3.14) but with $2\varepsilon_v$ replaced by what he calls d and refers to as the 'mean free path'. (Takayasu's equation (20)', but note that his $\alpha(r)$ corresponds to our $\alpha(\varepsilon)+1$].) This apparent discrepancy may well be due to different definitions of mean free path.

All the results in this paper are, we emphasise, for the one-dimensional random walks, in particular (3.13). So is Takayasu's (1982) result. Nevertheless Tsurumi and Takayasu (1986) have shown that equation (3.13) may be fitted remarkably well to the simulation results of Powles and Quirke (1984) and Rapaport (1984) (see also figure 9). However Tsurumi and Takayasu did not have independent values of d which they used as a fitting parameter. In fact Powles (1985) also measured ε_v in his simulations. The fitted value of d corresponds to $2\varepsilon_v$ to about 20%. It would seem, therefore, that equation (3.13), with $2\varepsilon_v$, is quite a good fit, at least for this state, for a realistic (simulated but three-dimensional) liquid. The agreement is all the more remarkable because the actual $\phi_v(t)$ is not remotely like an exponential.

Finally, formula (3.13) was found by Matsuura *et al* (1986) to fit remarkably well in a finite-fractal analysis of the trajectories of latex suspensions of polystyrene spheres and of the motion of bacteriophage T4 particles in solution by direct observation. However, no test was made as to whether the parameter $2\varepsilon_v$ in (3.13) is correct for these three-dimensional macroscopic trajectories.

4. Crystals, liquids and gases

Although our model is rather crude, apart from being one dimensional, it appears, as discussed in § 3, to be moderately realistic for realistic liquids and suspensions for $p \simeq 1$. We may expect the same to be true for gases since liquids can change continuously to gases by a suitable path in the (P, T) diagram. As already noted, for $p \to 1$ we have a model for a perfect gas.

We noted in § 3 that for $p \to 0$ the model corresponds to a particle in a box which is an approximation for an atom in a perfect crystal. However, in a real crystal the atoms can diffuse, albeit slowly, and if we had a long enough trajectory we still ought to observe a fractal 'tail' with $\alpha \to 1$ which is predicted by (3.12) for p small (see figure 8).

What is not observed in nature is the case $p = \frac{1}{2}$ which we call the 'mathematical fluid'. Even for macroscopically large 'Brownian' particles in solution the changeover to $\alpha \to 0$ must be observed if ε is small enough. It is not normally observed because such an ε would have to be of microscopic dimensions. So what is normally regarded as Brownian motion is analogous to the 'real liquid', but one which is only observed for such large values of ε that the curved part of the plot is not measured and such that the shift in the asymptotic line with $\alpha \sim 1$ is negligible in the observations.

A crystal cannot change continuously to a liquid. It is a first-order phase transition. In our model this corresponds to not being able to go continuously (by increasing p from $p \simeq 0$) from 'real crystal' to 'real liquid' without passing through a non-physical state, the 'mathematical fluid'. An idealised diagram illustrating these remarks is given in figure 8.

We have already reported finite-fractal plots for a simulated Lennard-Jones 12-6 (sp 2.5) fluid at a typical liquid state point. Since the vapour pressure of this fluid is known (Powles 1984) the coexisting vapour at the same temperature can be readily

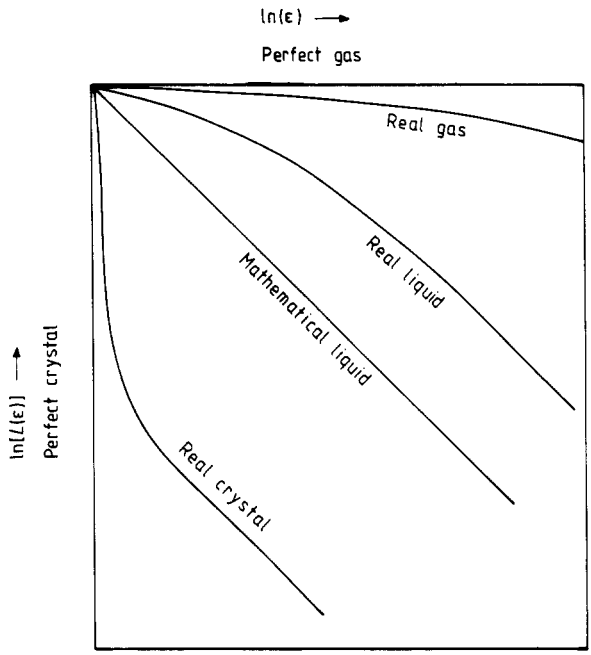

Figure 8. Diagrammatic representation of equation (3.12) for various values of the persistence probability, p, as described in the text.

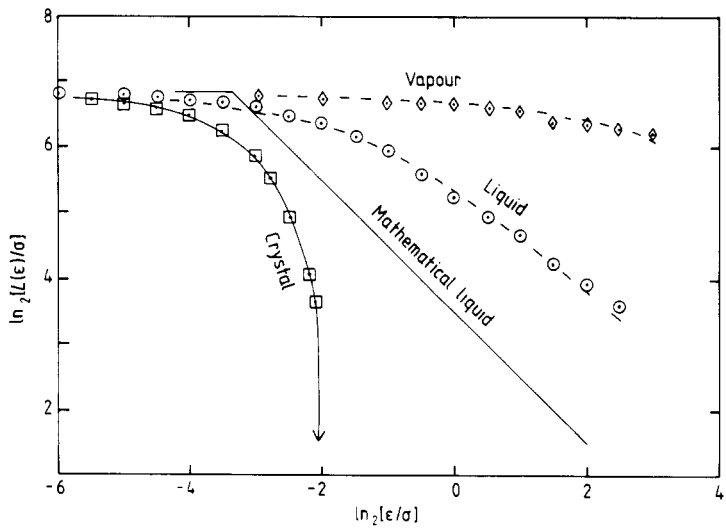

Figure 9. Simulation results for particles interacting with a Lennard-Jones 12-6 sp 2.5 potential. The three sets of points are for the liquid, the coexisting vapour and the crystal, respectively, all at the same temperature, 0.93 kT/ε. Note that the liquid is not at the triple point and the crystal is under substantial pressure ($P \simeq 10\varepsilon/\sigma^3$). σ is the length parameter in the potential and is effectively the atomic diameter. The broken curves for liquid and vapour are for equation (3.13) and the curve for the crystal merely guides the eye.

simulated for the same number of simulation steps as for the liquid. The result of the finite-fractal analysis is shown in figure 9. We are even further from the limiting behaviour of α, because for the vapour τ_v and ε_v are about 25 times larger than for the liquid.

It is also possible to simulate the (FCC) crystal *at the same temperature* by increasing the pressure (actually by choosing a high enough density in the 'microcanonical' simulation). This is slightly arbitrary but the density chosen is about that which would be suitable for a real argon crystal. This density and temperature are such that D is many orders of magnitude smaller than for the liquid. Indeed it is not measurable for any reasonable simulation length. Thus our simulations were not long enough to reveal in figure 9 the lower part of the curve for 'real crystal' in the diagram of figure 8. In fact this curve for the crystal in figure 9 falls precipitously to negative ordinates for a very small further increase in ε. The critical value of ε is about $\sigma/4$ which is about the expected value for the amplitude of vibration of an atom in the crystal lattice. Note that $\alpha(\varepsilon)$ for the crystal is greater than unity for the largest values of ε.

Notice that in figure 9, L_c, i.e. $L(\varepsilon \to 0)$, is the same for all three states, crystal, liquid and vapour. This is so because (recall $L_c = \langle v \rangle T$) $\langle v \rangle$ for a classical system is independent of the state at a given temperature and the three simulations were of the same duration, T.

As a guide to the eye we have included a straight line corresponding to $\alpha = 1$, with the knee to $\alpha = 0$ at a somewhat arbitrary position, marked 'mathematical liquid' (cf figure 2). When the crystal melts the finite-fractal plot 'jumps over' this line.

We shall report on the behaviour of this and other models in three dimensions elsewhere (Powles and Fowler 1986).

Acknowledgment

JGP thanks the Science and Engineering Research Council for encouragement.

Appendix 1. Proof of equation (3.4)

Let $p_\pm(x, t)$ be the probability flowing into the point (x, t) from $(x \mp l)$ at time $(t - \tau)$. Then

$$p_\pm(x, t+\tau) = pp_\pm(x \mp l, t) + qp_\mp(x \pm l, t).$$

Use units of l and τ, write $\mathscr{F}[[p(x, t)] = p(k, t)$ and recall that $\mathscr{F}[f(x \pm l)] = \exp(\pm ikl)\mathscr{F}[f(t)]$. Then

$$p_\pm(k, m+1) = p \exp(\mp ik)p_\pm(k, m) + q \exp(\pm ik)p_\mp(k, m).$$

This difference equation has a solution of the form

$$p_\pm(k, m) = \sum_{i=1}^{2} A_{\pm i}(k)\alpha_i^m.$$

Hence (after cancelling α^m)

$$A_\pm \alpha = p \exp(\mp ik)A_\pm + q \exp(\pm ik)A_\mp.$$

We have $A_{\pm}=0$ unless

$$[\alpha - p\exp(-ik)][\alpha - p\exp(ik)] = q^2$$

i.e.

$$\alpha_{1,2} = p\cos k(+,-)[p^2\cos k - (p-q)]^{1/2}.$$

At $t=0$, the particle is definitely at the origin and is equally likely to be moving in either direction. Hence $p_{\pm}(x,0)=\frac{1}{2}\delta(x)$, so that $p_{\pm}(k,0)=\frac{1}{2}$, and

$$A_{\pm 1}(k) + A_{\pm 2}(k) = \tfrac{1}{2}.$$

For $m=1$ $(\tau \leqslant t < 2\tau)$

$$p_{\pm}(x,1) = \tfrac{1}{2}\delta(x \mp 1)$$

so that

$$p_{\pm}(k,1) = \tfrac{1}{2}\exp(\mp ik).$$

Hence

$$A_{\pm 1}(k)\alpha_1 + A_{\pm 2}(k)\alpha_2 = \tfrac{1}{2}\exp(\mp ik).$$

Therefore

$$A_{\pm 1,2}(k) = (-,+)\tfrac{1}{2}[\alpha_{2,1} - \exp(\mp ik)]/(\alpha_1 - \alpha_2)$$

so that $p(k,t) = p_+(k,t) + p_-(k,t)$ is determined. But

$$\frac{\langle x^2(t)\rangle}{l^2} = -\frac{\partial^2}{\partial k^2}p(k,t)|_{k=0}.$$

Hence, after some algebra,

$$\frac{\langle x^2(t)\rangle}{l^2} = m\left(\frac{p}{q}\right) - \frac{(p-q)}{2q^2} + \frac{(p-q)}{2q^2}(p-q)^m$$

which is (3.4).

Appendix 2. Proof of equation (3.12)

By reference to figure 5 it is clear that

$$p_+(x, t+1) = pp_+(x-1, t) + qp_-(x+1, t)$$

and

$$p_-(x, t+1) = pp_-(x+1, t) + qp_+(x-1, t)$$

where $p_{\pm}(x,t)$ is the probability of displacement to the right (or left) at position x, in units of l, at time t in units of τ. The boundary conditions are

$$p_{\pm}(x,0) = \tfrac{1}{2}\delta_{x,0} \qquad p_+(-n,t) = p_-(n,t) = 0 \qquad \text{for all } t$$

for evaluation of $L(nl)$. It is convenient to put $\varepsilon/l = n = (r+1)$. Then the probability 'absorbed' at $(r+1)$ at $(t+1)$ on the right is $pp_+(r,t)$ and on the left is $pp_-(-r,t)$. But $p_-(-r,t) = p_+(r,t)$ so that the probability absorbed at $(t+1)$ is proportional to $p_+(r,t)$.

It is also convenient to evaluate $L(\varepsilon)/L_c$ in a different way from that described in § 2.2, equation (2.10). For each rectilinear step of length ε along the trajectory the corresponding contour length, ΔL_{ci}, depends on the step i in question. For a trajectory of indefinite length we have

$$L(\varepsilon)/L_c = \varepsilon/\langle \Delta L_c \rangle$$

where $\langle \Delta L_c \rangle$ is the mean contour length for a step. But every trajectory terminating at time $(t+1)$ has a contour length $(t+1)l$ with probability proportional to $p_+(r, t)$ so that

$$\langle \Delta L_c \rangle = \sum_{t=0}^{\infty} (t+1) p_+(r, t) \left(\sum_{t=0}^{\infty} p_+(r, t) \right)^{-1}$$

$$= 1 + \sum t p_+(r, t) \left(\sum p_+(r, t) \right)^{-1} \qquad \text{for } \varepsilon/l = (r+1).$$

Put $S_\pm(x, u) \equiv \Sigma_{t=0}^{\infty} p_\pm(x, t) u^t$. Then

$$\langle \Delta L_c \rangle = 1 + (\partial S_+(r, u)/\partial u)/S_+(r, u)|_{u=1}.$$

We therefore evaluate $S_+(r, u)$. We have

$$\sum_{t=0}^{\infty} p_\pm(x, t+1) u^t = u^{-1}\{(S_\pm(x, u) - p_\pm(x, 0))\}$$

so

$$S_\pm(x, u) - p_\pm(x, 0) = u\left\{ \binom{p}{q} S_+(x-1, u) + \binom{p}{q} S_-(x+1, u) \right\}.$$

Put

$$R_\pm(y, u) \equiv \sum_{x=-r}^{r} S_\pm(x, u) y^x.$$

Then

$$\sum_{x=-r}^{r} S_+(x-1, u) y^x = y R_+(y, u) - y S_+(r, u) y^r$$

since $S_+(-r-1, u) = 0$.

Similarly

$$\sum_{x=-r}^{r} S_-(x+1, u) y^x = y^{-1} R_-(y, u) - y^{-1} S_-(-r, u) y^{-r}.$$

Now using

$$\sum_{-r}^{r} p_\pm(x, 0) y^x = \tfrac{1}{2} \qquad S_-(-r, u) = S_+(r, u)$$

we find

$$R_\pm(y, u) - \tfrac{1}{2} = u\left\{ \binom{p}{q} y[R_+(y, u) - S_+(r, u) y^r] + \binom{p}{q} y^{-1}[R_-(y, u) - S_+(r, u) y^{-r}] \right\}.$$

Hence

$$y^r R_+(y, u) = y^r R_-(y^{-1}, u)$$

$$= \frac{y^{r+1}\{\tfrac{1}{2}[1 - u(p-q)/y] - u S_+(r, u)[(1 - up/y)(p y^{r+1} + q y^{-r-1}) + (uq/y)(q y^{r+1} + p y^{-r-1})]\}}{[1 + u^2(p-q)] - up(y^2+1)}.$$

We require only $S_+(r, u)$. Now the left-hand side of the above equation is a polynomial in y of degree $2r$. Hence the right-hand side must also be a polynomial in y of degree $2r$. Hence the numerator on the right-hand side must contain the factors $(y-\alpha)(y-\beta)$ where α, β are the roots of the quadratic in y in the denominator. Hence

$$S_+(r, u) = \frac{\frac{1}{2}[1-u(p-q)/y]}{u\{(1-up/y)(py^{r+1}+qy^{-r-1})+(uq/y)(qy^{r+1}+py^{-r-1})\}}$$

when $y=\alpha$ or β, where these are the solutions of

$$y^2-(up)^{-1}[1+u^2(p-q)]y+1=0$$

so that

$$\alpha\beta=1 \qquad (\alpha+\beta)=(up)^{-1}[1+u^2(p-q)].$$

To see that the two roots lead to the same form of $S_+(r, u)$ one can write $S_+(r, u)$ in a more symmetrical form. Multiply numerator and denominator by $[1-u(p-q)y]$ and use the quadratic equation. A little algebra then leads to

$$S_+(r, u) = \frac{1-u^2(p-q)^2}{u\{(y^{r+1}+y^{-r-1})[1-u^2(p-q)^2]-up(p-q)(y^{r+1}-y^{-r-1})(y-y^{-1})\}}.$$

Then whether one takes $y=\alpha$ or $y=\beta$ one finds

$$S_+(r, u) = \frac{1-u^2(p-q)^2}{u\{(\alpha^{r+1}+\beta^{r+1})[1-u^2(p-q)^2]-up(p-q)(\alpha^{r+1}-\beta^{r+1})(\alpha-\beta)\}}.$$

Other equivalent forms are

$$S_+(r, u) = \frac{1-\frac{1}{2}u(p-q)(\alpha+\beta)}{u[(\alpha^{r+1}+\beta^{r+1})-u(p-q)(\alpha^r+\beta^r)]}$$

and

$$S_+(r, u) = \frac{\frac{1}{2}(a-\beta)}{(a^{r+1}-\beta^{r+1})-u(\alpha^r-\beta^r)}.$$

Putting $u=1-\delta$, $\delta>0$, we find, with frequent use of $(p+q)=1$ and lengthy algebra, that

$$S_+(r, 1)=\tfrac{1}{2}$$

and

$$\frac{\partial S_+(r, u)}{\partial u}(S_+(r, u))^{-1}\bigg|_{u=1} = -\frac{1}{2}\frac{\partial S_+(r, 1-\delta)}{\partial \delta}\bigg|_{\delta=0}$$
$$= r+r(r+1)(q/p).$$

Hence

$$\langle \Delta L_c \rangle = (1+r)[1+r(q/p)]$$

and, since $\varepsilon/l=(1+r)$,

$$L(\varepsilon)/L_c=[(\varepsilon/l)(q/p)+(p-q)/p]^{-1}.$$

This is the same as equation (3.12), given that $q=1-p$. The special cases, (3.13), etc, follow immediately.

References

Chandrasekhar S 1943 *Rev. Mod. Phys.* **15** 1
Fürth R 1917 *Ann. Phys., Lpz.* **53** 177
Hausdorff F 1919 *Math. Ann.* **79** 157
Kalia R K, de Leeuw S W and Vashishta P 1985 *J. Phys. C: Solid State Phys.* **18** L905
Mandelbrot B B 1982 *The Fractal Geometry of Nature* (San Francisco: Freeman)
Matsuura S, Tsurumi S and Imai N 1986 *J. Chem. Phys.* **84** 539
Powles J G 1984 *Physica* A **126** 289
—— 1985 *Phys. Lett.* **107A** 403
Powles J G and Fowler R F 1986 *Physica* A submitted for publication
Powles J G and Quirke N 1984 *Phys. Rev. Lett.* **52** 1571
Rahman A 1964 *Phys. Rev.* **136** A405
Rapaport D C 1984 *Phys. Rev. Lett.* **53** 1965
—— 1985 *J. Stat. Phys.* **40** 751
Richardson L F 1961 *General Systems Year Book* **6** 139
Takayasu H 1982 *J. Phys. Soc. Japan* **51** 3057
Toxvaerd S 1985 *J. Chem. Phys.* **82** 8658
—— 1986 *Phys. Lett.* **114A** 159
Tsurumi S and Takayasu H 1986 *Phys. Lett.* **113A** 449
van Beijeren H 1982 *Rev. Mod. Phys.* **54** 195
Vashishta P, Ebbsjo I, Kalia R K and de Leeuw S W 1985 Private communication